JGSP **8** (2006) 1–16

JOURNAL OF
Geometry and Symmetry
in Physics

CLOSED GEODESICS ON CERTAIN SURFACES OF REVOLUTION

JAMES C. ALEXANDER

Communicated by John Oprea

Abstract. Recently I. Mladenov and J. Oprea have investigated a number of surfaces of revolution, and in particular, developed numerical shooting methods to investigate geodesics on those surfaces, which in turn led them to raise some questions concerning closed geodesics on those surfaces. Here we develop explicit formulae, usually in terms of elliptic integrals, that permit us to answer the questions. The computations are based of course on the classical Clairaut's formulae, and a major point is to demonstrate that explicit computations can be made. A closed geodesic on a surface of revolution oscillates q times across the equator of the surface, while winding p times around the axis of rotation. Call the pair (p, q) the *type* of the geodesic. In particular, the permitted types are explicitly determined for the investigated surfaces.

1. Introduction

Recently I. Mladenov and J. Oprea have considered some particular surfaces of revolution [8–10], characterizing them via variational principles, and also considered geodesics on them. They developed Maple code for visualization and other computation. In particular, they coded a shooting method to construct closed geodesics. Motivated by this work, especially of [9], our purpose here is to demonstrate how explicit calculations can be done. For many surfaces, including those investigated by Mladenov and Oprea [8,9], we develop explicit formulas, in terms of complete elliptic integrals. For others, including the Hopf surfaces in [10], the treatment is slightly different.

The surfaces we consider are rotated around the z-axis and are symmetric with respect to the xy-plane (although this last is not necessary). The 'equator' in the xy-plane is a geodesic. Other geodesics intersect the equator. A closed geodesic winds around the z-axis p times while making q oscillations across the equator (hence $2q$ intersections). We explicitly determine the permitted p and q, and in

most cases characterize the associated geodesics by the angle they make with the equator.

The theory and methods are classical. Everything about geodesics on surfaces of revolution follows from investigations of Alexis Clairaut (1713–1765), and can be found in many books on differential geometry, e.g., [11]. Our explicit calculations are in terms of complete elliptic integrals, which are also classic. We use the book of Byrd and Friedman [2] as our reference. A brief Appendix is included here. The purpose of the current paper is to illustrate by cases how calculations can be effected.

2. Surfaces

Consider a (smooth) curve Γ: $x = h(u)$, $z = g(u)$ in the xz-plane, with the following properties: $h(-u) = h(u)$, $h(u) \geq 0$, $g(-u) = -g(u)$, $g(u) \geq 0$, $h'(0) = 0$, $h'(u) < 0$ for positive g (although we relax some of these conditions below). Let $\gamma^2(u) = h'(u)^2 + g'(u)^2$ be the square of the element of arclength. Note (useful below) that h can be inverted to give $u = u(h)$ as a function of h. We consider the surface Σ obtained by rotating Γ about the z-axis:

$$x = h(u_2)\cos u_1, \qquad y = h(u_2)\sin u_1, \qquad z = g(u_2).$$

Thus u_1 is the revolution angle – the longitude – and $u_2 = u$, the latitude. Such a parametrization is called a Clairaut parametrization. In particular, we are interested in geodesics on the surface, and more particularly, closed geodesics.

2.1. Examples of Surfaces

1. *Sphere*: $h(u) = r\cos u$, $g(u) = r\sin u$, $\gamma(u) \equiv r$.
2. *Spheroid* (See [3, Exercise 8, p. 108 and Exercise 4, p. 446]): $h(u) = a\cos u$, $g(u) = b\sin u$, $\gamma^2(u) = a^2\sin^2 u + b^2\cos^2 u$.
3. *Rotated cycloid* (Figure 1): $h(u) = a(1+\cos u)$, $g(u) = a(u+\sin u)$, $\gamma^2(u) = 2a^2(1+\cos u) = 2ah(u)$.
4. *Generalized Mylar balloon* (see [8]): $h(u) = r\,\mathrm{cn}(u,k)$, $g(u)$ complicated, $\gamma(u) = r\sqrt{1-k^2}$. Here $\mathrm{cn}(u,k)$ is the Jacobian elliptic cosine function with modulus $k < 1$ ($k = 1/\sqrt{2}$ is the original balloon).
5. *Unduloid* (see [9]) (Figure 2): $h(u) = a\sqrt{1+\epsilon^2+2\epsilon\sin u}$, $0 < \epsilon < 1$, $g(u)$ complicated, $\gamma(u) \equiv a$.
6. *Torus* (see [1]): $h(u) = \rho + a\cos u$, $g(u) = a\sin u$, $\gamma(u) \equiv a$.

7. *Hopf surface*: A Weingarten surface with relation $k_2 = ck_1 - d$ between its principle curvatures k_1, k_2 with $c \geq 1$, $0 \leq d < c/r_0$, where $r = 0$ is the equatorial radius [4], see also [6] (with figures). In this case, the parametrization is slightly different. These surfaces with $d = 0$ are characterized by a "moment variational principal" in [10]. The case $d = 0$, $c = 2$ is the Mylar balloon of [8].

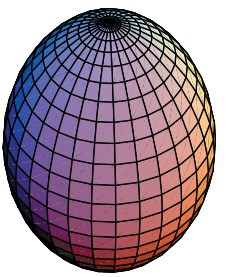

Figure 1. Rotated cycloid.

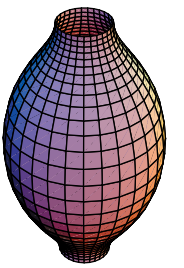

Figure 2. Unduloid with $\epsilon = 0.5$.

2.2. Geodesics

Geodesics on such a surface of rotation have a simple general structure. The curve (circle) generated by rotating the point given by $g(u) = 0$, i.e., $z = 0$, is a geodesic, which we call the *equator*. A *meridian* is a curve $u_1 =$constant. Any meridian is perpendicular to the equator. For any geodesic ζ and a point p on ζ, with coordinates (u_1, u_2), let ψ be the angle between ζ and the meridian through p. There is a constant $c = c_\zeta$ depending on ζ, such that for all p on ζ, the equality $h(u_2) \sin \psi = c$ holds. This is called Clairaut's relation and contains all the geometric information about the geodesic.

Any non-equatorial geodesic ζ oscillates back and forth across the equator, as it also encircles the z-axis. The geodesic inherits the rotational and symmetric symmetries of the surface – that is, it looks the same forwards and backwards, and on reflection through the equator. The geodesics can be parametrized up to rotation in several ways. One is by the crossing angle $\theta = \theta_c$ at which it crosses the equator (the *angle of elevation*). A second is the Clairaut value $c = c_\zeta$. This is the minimum of h for points on ζ – the distance of ζ to the axis of rotation. By

Clairaut's relation, if h_0 is the radius of the equator (a notation used throughout), $c = h_0 \cos\theta$. We denote the geodesic ζ_c or $\zeta_\theta = \zeta_{c(\theta)}$.

3. Results

Thus non-equatorial, non-meridinal closed geodesics ζ determine a pair of positive coprime integers p and q as noted above. That is, it winds around the z-axis p times while making q oscillations across the equator. Call the pair (p, q) the *type* of the geodesic.

Theorem 1. *The range of types p/q of closed geodesics for various surfaces is given in* Table 1. *That is, a pair (p, q) is the type of a closed geodesic if and only if the ratio p/q is in the indicated interval.*

If the surface is smooth at $g(u) = 0$, the interval of possible p/q includes 1 (realized by meridians). In all cases except the sphere, and possibly Hopf surfaces, the function I_c defined below is strictly monotonic, so up to rotation, there is a unique geodesic for each permissible p/q. Here this is demonstrated graphically, and follows from the explicit formulae developed in Section 4. Details are left to the reader. The computations are not as complete for Hopf surfaces, and the verification will required additional analysis.

Proposition 2. *For each surface there is a function of c (or θ)*

$$I_c(\text{ or } I_\theta) = \int_{\psi_0}^{\pi/2} 2\tan\psi \,\mathrm{d}u_2 = -\int_c^{h_0} \frac{2c\gamma\big(u(h)\big)}{h\sqrt{h^2-c^2}} \frac{\mathrm{d}u}{\mathrm{d}h}\,\mathrm{d}h = -\int_c^{h_0} \frac{2c\gamma(h)}{h\sqrt{h^2-c^2}}\,\mathrm{d}h$$

that measures the u_1 increment Δu_1 between oscillations across the equator ζ_c.

The first integral is a line integral along ζ_c and the second or third is how we compute. Note that we have used the inversion $u(h)$ of h, so $\mathrm{d}u/\mathrm{d}h = (\mathrm{d}h/\mathrm{d}u)^{-1}$ and $\gamma = \gamma\big(u(h)\big)$. Moreover, it is possible to determine the range of I_c, so the possible p and q are characterized, see Theorem 1. In the remainder of this paper, we develop I_c and then consider it in more detail for each example.

Corollary 3. *A geodesic ζ_c is closed, with type (p, q), if and only if $I_c/\pi = p/q$.*

Table 1. Ratios p/q of types of closed geodesics.

Surface	Range	Comments
Sphere	$\{1\}$	All geodesics are great circles.
Spheroid	$(b/a, 1]$ or $[1, b/a)$	Depending on whether the spheroid is oblate or prolate.
Rotated cycloid	$[1, 1/\sqrt{2})$	
Generalized Mylar balloon	$(k, 1]$	$k = 1/\sqrt{2}$ is the standard Mylar balloon.
Unduloid	$(1/\sqrt{\epsilon}, \infty)$	Thus in answer to a question of Mladenov and Oprea [9], the closed geodesic with $p/q = 2/1$ exists for $\epsilon > 1/4$.
Torus	$\left(\sqrt{\frac{a}{\rho + a}}, \infty\right)$	Because the torus has genus 1, there is a second set of closed geodesics, one for each rational p/q.
Hopf surface	$(1/\sqrt{c - dr_0}, 1]$ or $[1, 1/\sqrt{c - dr_0})$	$d = 0$, $c = 1/k$ are the generalized Mylar balloons of [10].

Proof of Proposition 2: By standard formulae of the differential geometry of surfaces Σ, the metric tensor (first fundamental form) is

$$\begin{pmatrix} E & F \\ F & G \end{pmatrix} = \begin{pmatrix} h^2(u) & 0 \\ 0 & \gamma^2(u) \end{pmatrix}$$

and thus the geodesic equations are

$$\ddot{u}_1 + 2\frac{h'(u_2)}{h(u_2)}\dot{u}_1\dot{u}_2 = 0$$

$$\ddot{u}_2 - \frac{h(u_2)h'(u_2)}{\gamma^2(u_2)}\dot{u}_1\dot{u}_1 + \frac{\gamma'(u_2)}{\gamma(u_2)}\dot{u}_2\dot{u}_2 = 0.$$

Here the dot derivative is with respect to arc length. These equations can be integrated once. Let $v_i = \dot{u}_i$. The first equation is $\dot{v}_1 h + 2v_1\dot{h} = 0$, so $v_1 = c/h^2$, where c is a constant of integration. Substituting in the second equation and multiplying by $2\gamma^2 v_2$, the second equation yields $\gamma^2 v_2^2 = c' - c^2/h^2$. To have a geodesic of unit speed

$$v_1^2 E + v_2^2 G = v_1^2 h^2 + v_2^2 \gamma^2 = 1$$

so that $c' = 1$, and thus we obtain

$$v_1 = \frac{c}{h^2}, \qquad v_2 = \frac{1}{\gamma}\sqrt{1 - \frac{c^2}{h^2}}.$$

Denote this geodesic ζ_c. Note that $v_2 = 0$ on ζ_c when $h = c$, and that c is the radial distance from the z-axis at which this happens. Note that

$$\begin{aligned}\frac{\mathrm{d}^2 u_2}{\mathrm{d}u_1^2} &= \frac{\mathrm{d}}{\mathrm{d}u_1}\left(\frac{\dot{u}_2}{\dot{u}_1}\right) = \frac{1}{\dot{u}_1}\left(\frac{\dot{u}_1\ddot{u}_2 - \dot{u}_2\ddot{u}_1}{\dot{u}_1^2}\right) \\ &= \frac{hh'}{\gamma^2} + 2\gamma'\gamma\left(\frac{\dot{u}_2}{\dot{u}_1}\right)^3 + 2\frac{h'}{h}\left(\frac{\dot{u}_2}{\dot{u}_1}\right)^2 < 0\end{aligned}$$

when $v_2 = \dot{u}_2$, since $h' < 0$. Hence ζ_c has a strict u_2 maximum. Also note that Clairaut's relation follows from the fact that $\sin\psi = \sqrt{E}v_1 = hv_1$. Now consider the distance between the equatorial crossing point of ζ_c and its u_2 maximum:

$$\begin{aligned}u_1\Big|_{u_2=0}^{h(u_2)=c} &= \int_{u_2=0}^{h(u_2)=c} \mathrm{d}u_1 = \int_{h_0}^{c} \frac{\mathrm{d}u_1}{\mathrm{d}t}\frac{\mathrm{d}t}{\mathrm{d}u_2}\frac{\mathrm{d}u_2}{\mathrm{d}h}\,\mathrm{d}h \\ &= \int_{h_0}^{c} \frac{\dot{u}_1}{\dot{u}_2}\frac{\mathrm{d}u_2}{\mathrm{d}h}\,\mathrm{d}h = -\int_{c}^{h_0} \frac{c\gamma}{h\sqrt{h^2 - c^2}}\frac{\mathrm{d}u}{\mathrm{d}h}\,\mathrm{d}h.\end{aligned}$$

Here $\gamma = \gamma\big(u(h)\big)$. This completes the proof of Proposition 2.

Proof of Corollary 3: The function I_c is twice this integral. When $2I_c$ is a rational multiple p/q of 2π, ζ_c closes up after q full oscillations across the equator ($2q$ crossings) and encircling the z-axis p times.

Theorem 1 is proved by calculations in Section 4. Note that, since $h' = 0$ at h_0, the integral is improper at both limits. How accessible this integral is depends on what $\gamma\big(u(h)\big)$ and $\mathrm{d}u/\mathrm{d}h = (\mathrm{d}h/\mathrm{d}u)^{-1}$ look like. The integral can usually be computed numerically – the singularities at the limits are reasonable ($-1/2$ powers). In favorable cases, I_c can be explicitly computed, below in terms of elliptic integrals. Properties of I_c are known in some circumstances.

Proposition 4. *If* $\lim_{h\to 0} g'(u) = 0$*, then* $\lim_{c\to 0} I_c = \pi$.

This of course is expected for geometric reasons.

Proof: If $g'(u) = 0$, then $-\gamma \mathrm{d}u/\mathrm{d}h \to 1$. Given $\epsilon > 0$, choose $\bar{c} = \bar{c}(\epsilon)$ so that $1 - \epsilon < -\gamma \mathrm{d}u/\mathrm{d}h < 1 + \epsilon$ for $0 \le h \le \bar{c}$. Consider

$$-\int_c^{h_0} \frac{2c\gamma \frac{\mathrm{d}u}{\mathrm{d}h}\,\mathrm{d}h}{h\sqrt{h^2 - c^2}} = -\int_c^{\bar{c}} \frac{2c\gamma \frac{\mathrm{d}u}{\mathrm{d}h}\,\mathrm{d}h}{h\sqrt{h^2 - c^2}} - c\int_{\bar{c}}^{h_0} \frac{2\gamma \frac{\mathrm{d}u}{\mathrm{d}h}\,\mathrm{d}h}{h\sqrt{h^2 - c^2}}.$$

The final integral is uniformly bounded in c, so as $c \to 0$, the final term disappears. On the other hand

$$(1-\epsilon)\int_c^{\bar{c}} \frac{2c\gamma \frac{\mathrm{d}u}{\mathrm{d}h}\,\mathrm{d}h}{h\sqrt{h^2 - c^2}} < \int_c^{\bar{c}} \frac{2c\,\mathrm{d}h}{h\sqrt{h^2 - c^2}} < (1+\epsilon)\int_c^{\bar{c}} \frac{2c\gamma \frac{\mathrm{d}u}{\mathrm{d}h}\,\mathrm{d}h}{h\sqrt{h^2 - c^2}}$$

and the integrals on the extremes evaluate to $\pi - 2\arcsin(c/\bar{c})$. These estimates prove the claim.

Proposition 5. *Let subscript '0' denote values when $g = 0$ (the equator). If $h_0' = 0$, then*

$$\lim_{c \to h_0} I_c = \frac{\pi\gamma_0}{\sqrt{-h_0 h_0''}}.$$

This is also expected and the limiting value of I_c is twice the distance between conjugate points on the equator, which is determined from the Jacobi equation along the equator.

Proof: Write $h = h_0 + \frac{1}{2}h_0''(u-u_0)^2 + \frac{1}{2}x(u-u_0)^2$, where $x \to 0$ as $u \to 0$ (or equivalently $h \to h_0$), so that $u - u_0 = \sqrt{-2(h_0 - h)/(h_0'' + x)}$. Besides $c = h_0 - \epsilon$ and $\tilde{h} = h_0 - h$. Thus

$$\begin{aligned} I_c &= \int_0^{\epsilon} \frac{2(h_0-\epsilon)\gamma}{h_0\sqrt{2h_0}\sqrt{\epsilon - \tilde{h}}} \frac{\mathrm{d}\tilde{h}}{\sqrt{-2(h_0'' + x)\tilde{h}}} \\ &= \frac{(h_0-\epsilon)\tilde{\gamma}}{h_0\sqrt{h_0}} \frac{1}{\sqrt{-(h_0'' + \tilde{x})}} \int_0^{\epsilon} \frac{\mathrm{d}\tilde{h}}{\sqrt{\tilde{h}(\epsilon - \tilde{h})}} = \frac{\pi\tilde{\gamma}(h_0 - \epsilon)}{h_0\sqrt{-h_0(h_0'' + \tilde{x})}} \end{aligned}$$

where $\tilde{x}$ is an intermediate value of x and $\tilde{\gamma}$ is an intermediate value of γ. Let $\epsilon \to 0$ to obtain the result.

Proposition 6. *The derivative of I_c is*

$$\frac{\mathrm{d}I_c}{\mathrm{d}c} = -\int_c^{h_0} \frac{h_0(h^2 - c^2 - ch)\gamma}{h^2(c+h)(h_0 - c)\sqrt{h^2 - c^2}} \frac{\mathrm{d}u}{\mathrm{d}h}\,\mathrm{d}h.$$

This expression can be evaluated in favorable cases to show, for example, that I_c is monotonic. However, it is usually easier to differentiate the explicit expression for I_c.

Proof: Let $\tilde{h} = (h - c)/(h_0 - c)$. Substituting in I_c removes c from the limits of integration. Differentiate with respect to c, and substitute back.

4. Computations

The remainder of the paper consists of explicit computations, which yield Theorem 1, and also contain addition precision.

0. *Cone* (non-elliptic warm up): A cone, generated by $h(u) = r - u$, $g(u) = mu$, does not satisfy the condition $h'(0) = 0$ but the integral makes sense, and is a straightforward computation:

$$I_c = 2\sqrt{1 + m^2}\arccos(c/r) = 2\csc(\phi/2)\arccos(c/r)$$

where ϕ is the angle at the cone point – a fact that can be seen geometrically, since the cone is developable, i.e., can be "opened up" to a sector of a disk preserving the metric.

1. *Sphere* (test case): In this case $u = \arccos(h/r)$, so $\mathrm{d}u/\mathrm{d}h = -1/\sqrt{r^2 - h^2}$. The integral I_c is "pseudo-elliptic" and can be antidifferentiated in terms of elementary functions with the change of variable $w = h^2$

$$I_c = \int_c^r \frac{2cr\,\mathrm{d}h}{h\sqrt{(r-h)(h-c)(h+c)(h+r)}} = \int_{c^2}^{r^2} \frac{cr\,\mathrm{d}w}{w\sqrt{(r^2-w)(w-c^2)}} = \pi$$

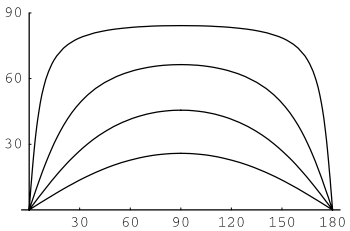

Figure 3. Upper half of geodesics (great circles) on a sphere in (u_1, u_2) coordinates (which are ordinary spherical coordinates). Values are in degrees. The bottom is the equator and the top (at $u_2 = 90°$) is the pole. In this case, all geodesics return to the equator with $\Delta u_1 = 180°$, but on other surfaces, Δu_1 is a function I_c of $c = h(u_{2,\mathrm{max}})$.

as we knew beforehand. See Figure 3.

2. *Spheroid*: Recall $h = a\cos u$, so $u = \arccos h/a$, and

$$\gamma = \sqrt{a^2\sin^2 u + b^2\cos^2 u} = \frac{1}{a}\sqrt{a^4 - (a^2-b^2)h^2}.$$

Note that $\lim_{c\to a} I_c/\pi = b/a$.

Sub case a. *Prolate spheroid*: $b > a$. Then

$$I_c = \int_c^a \frac{2c\sqrt{b^2-a^2}\sqrt{h^2 + \frac{a^4}{b^2-a^2}}\,\mathrm{d}h}{ah\sqrt{(h^2-c^2)(a^2-h^2)}}.$$

With the change of variable [2, #235.02]

$$\begin{aligned} I_c &= \int_{c^2}^{a^2} \frac{2c\sqrt{b^2-a^2}\sqrt{w + \frac{a^4}{b^2-a^2}}\,\mathrm{d}w}{ah\sqrt{(w-c^2)(a^2-w)}} \\ &= 2\frac{a^4 + c^2(b^2-a^2)}{a^2bc}\Pi\left(-\frac{a^2(a^2-c^2)}{b^2c^2}\middle|\frac{(b^2-a^2)(a^2-c^2)}{a^2b^2}\right) \end{aligned}$$

where $\Pi(n\,|\,m)$ is the complete Legendre elliptic integral of the third kind (see Appendix).

Sub case b. *Oblate spheroid*: $b < a$. We compute, [2, #234.02]

$$\begin{aligned} I_c &= \int_c^a \frac{2c\sqrt{a^4-(b^2-a^2)h^2}\,\mathrm{d}h}{ah\sqrt{(h^2-c^2)(a^2-h^2)}} = \int_{c^2}^{a^2} \frac{c\sqrt{a^2-b^2}\sqrt{\frac{a^4}{a^2-b^2} - w}\,\mathrm{d}w}{aw\sqrt{(w-c^2)(a^2-w)}} \\ &= \frac{2b^2c}{a\sqrt{a^4-(a^2-b^2)c^2}}\Pi\left(\frac{a^2(a^2-c^2)}{a^4-(a^2-b^2)c^2}\middle|\frac{(a^2-b^2)(a^2-c^2)}{a^4-(a^2-b^2)c^2}\right). \end{aligned}$$

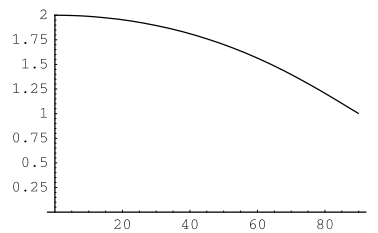

Figure 4. Graph of I_θ/π for prolate spheroid, $b/a = 2$.

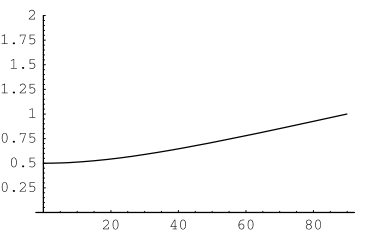

Figure 5. Graph of I_θ/π for oblate spheroid, $b/a = 1/2$.

The value of $I_c(\theta)$ is graphed in Figures 4 and 5 as a function of the crossing angle θ (in degrees) for $b = 2a$, and $a = 2b$.

3. *Rotated cycloid*: Here $\mathrm{d}u/\mathrm{d}h = \sqrt{h(2a-h)}$, so [2, #236.19, 336.01]

$$I_c = \int_c^{2a} \frac{2c\sqrt{2a}\,\mathrm{d}h}{h\sqrt{(2a-h)(h^2-c^2)}} = \frac{2c/a}{\sqrt{1+c/(2a)}} \prod\left(1 - \frac{c}{2a}\middle| \frac{1-\frac{c}{2a}}{1+\frac{c}{2a}}\right)$$

where again $\Pi(n\,|\,\kappa)$ is the complete Legendre elliptic integral of the third kind. The plot in Figure 6 shows $I_{c(\theta)}/\pi$ as a function of the crossing angle θ (in degrees).

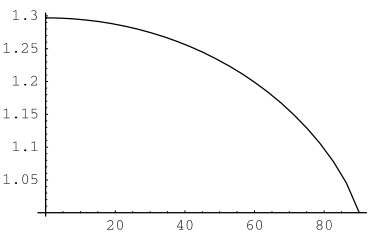

Figure 6. Graph of I_θ/π for rotated cycloid.

4. *Generalized Mylar Balloon*: Here $u = \mathrm{cn}^{-1}(h/r, k)$, [2, #128.01]

$$\frac{\mathrm{d}u}{\mathrm{d}h} = \frac{r\sqrt{1-k^2}}{\sqrt{(r^2-h^2)\left(h^2 + \frac{r^2(1-k^2)}{k^2}\right)}}.$$

With $w = h^2$, [2, #236.19, #336.01]

$$\begin{aligned} I_c &= \int_r^c \frac{r^2 c\sqrt{1-k^2}\,\mathrm{d}h}{h\sqrt{(h^2-c^2)(r^2-h^2)\left(h^2+\frac{r^2(1-k^2)}{k^2}\right)}} \\ &= \int_{c^2}^{r^2} \frac{r^2 c\sqrt{1-k^2}\,\mathrm{d}w}{2w\sqrt{(r^2-w)(w-c^2)\left(w+\frac{r^2(1-k^2)}{k^2}\right)}} \\ &= \frac{2c\sqrt{1-k^2}}{r} \prod\left(1 - \frac{c^2}{r^2}\middle| k^2\left(1-\frac{c^2}{r^2}\right)\right) \end{aligned}$$

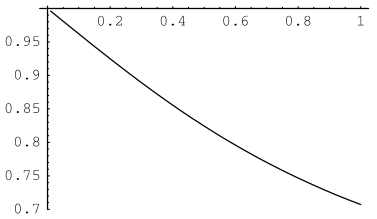

Figure 7. Graph of I_c/π for Mylar balloon, $k = 1/\sqrt{2}$.

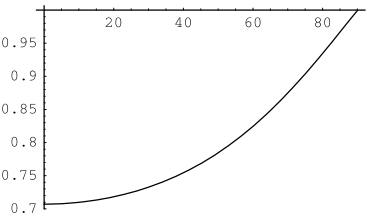

Figure 8. Graph of I_θ/π for Mylar balloon, $k = 1/\sqrt{2}$.

where again $\Pi(n \,|\, \kappa)$ is the complete Legendre elliptic integral of the third kind. The graph of Figure 7 is a plot of I_c/π against c/r for $k = 1/\sqrt{2}$ (the original Mylar balloon [8]). The graph of Figure 8 is a plot of $I_{c(\theta)}/\pi$ against the crossing angle θ (in degrees). For example there is such a geodesic associated with $I_c/\pi = 3/4 = 0.75$, $c/r = 0.785284\ldots$, and $\theta = 38.253\ldots^\circ$, corresponding to a value $u = \mathrm{cn}^{-1}(c/r)$ of $0.692602\ldots$. The computed value $u_0 = 0.691356\ldots$ of [9] agrees to within 0.2%.

5. *Unduloid*: Here

$$u = \arcsin\left(\frac{h^2 - a^2(1+\epsilon^2)}{2a^2\epsilon}\right)$$

and

$$\frac{\mathrm{d}u}{\mathrm{d}h} = -\frac{2h}{\sqrt{\big(a^2(1+\epsilon)^2 - h^2\big)\big(h^2 - a^2(1-\epsilon)^2\big)}}$$

so

$$I_c = \int_{\epsilon}^{a(1+\epsilon)} \frac{4ca\,\mathrm{d}h}{\sqrt{(h^2 - c^2)\big(a^2(1+\epsilon)^2 - h^2\big)\big(h^2 - a^2(1-\epsilon)^2\big)}}$$

whence, substituting $w = h^2$, [2, #257.00]

$$I_c = \frac{2}{\sqrt{\epsilon}} K\left(\frac{(1-\epsilon)^2\left((1+\epsilon)^2 - (c^2/a^2)\right)}{2\epsilon c^2/a^2}\right)$$

where $K(m)$ is the complete elliptic integral of the first type (see Appendix). For any $\epsilon < 1$, $I_c \to \infty$ as $c/a \to 1 - \epsilon$. The plot in Figure 9 displays $I_{c(\theta)}/\pi$ as a function of the parameter ϵ and the crossing angle θ (in degrees).

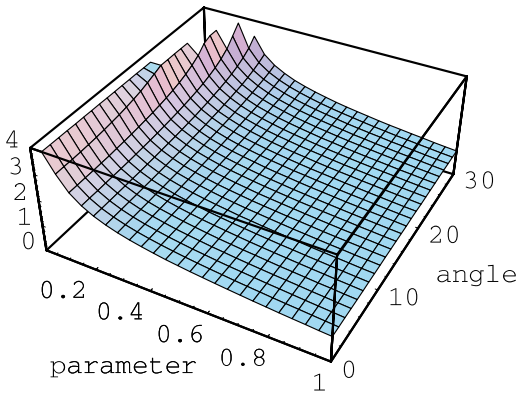

Figure 9. Graph of I_θ/π for unduloids with ϵ as parameter.

6. *Torus*: Here $u = \arccos\big((\rho-h)/a\big)$ and $\mathrm{d}u/\mathrm{d}h = 1/\sqrt{a^2-(\rho-h)^2}$, so

$$I_c = \int_c^{\rho+a} \frac{2ca\,\mathrm{d}h}{h\sqrt{\big((\rho+a)-h\big)\big(h-c\big)\big(h-(\rho-a)\big)\big(h+c\big)}}$$

which [2, #256.12, #340.01] yields

$$\begin{aligned} I_c =& \frac{2}{\rho-a}\sqrt{\frac{a}{c}}\Bigg[cK\left(\sqrt{\frac{\rho^2-(a-c)^2}{4ac}}\right) \\ &+ (\rho-a-c)\prod\left(\frac{(\rho-a)(\rho+a-c)}{2ac}\middle|\sqrt{\frac{\rho^2-(a-c)^2}{4ac}}\right)\Bigg]. \end{aligned}$$

Here $K(\kappa)$ is the complete elliptic integral of the first kind (see Appendix).

There is another set of geodesics on the torus; they wind around longitudinally. There is a second internal equator given by $u_2 = \pi$. Geodesics are of the type above for small θ. There is a critical angle $\arccos\big((\rho-a)/(\rho+a)\big)$ characterized by $c = \rho - a$, for which ζ_c is asymptotic to the internal equator. For larger θ (and $c < \rho - a$), the geodesic ζ_c crosses the internal equator and continues by symmetry. The order of parameters in [2, #256.12] is altered, which changes the evaluation of the integral. Thus the u_1 distance covered by ζ_c between the outer

and inner equator is [2, #256.12, #340.01]

$$I_c' = \frac{2a}{(\rho-a)\sqrt{\rho^2-(a-c)^2}}\left[(\rho-a)K\left(\sqrt{\frac{4ac}{(\rho^2-(a-c)^2}}\right)\right.$$
$$\left. -(\rho-a-c)\prod\left(\frac{2ac}{(\rho-a)(\rho+a-c)}\middle|\sqrt{\frac{4ac}{(\rho^2-(a-c)^2}}\right)\right].$$

Since these ζ_c do not oscillate, they are closed if I' is a rational multiple of π. If not, they are dense in the torus (there is one such geodesic for every rotation number, rational or not). The plots in Figure 10 and Figure 11 are plots of $I_{c(\theta)}/\pi$ and $I'_{c(\theta)}/\pi$ for a skinny torus, $a/\rho = 0.1$, and a fat torus, $a/\rho = 0.9$, as functions of the crossing angle θ (in degrees).

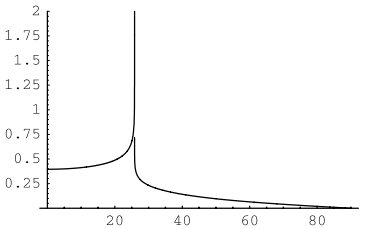

Figure 10. Graphs of I_θ/π and I'_θ/π for "skinny" torus, $a/\rho = 0.1$.

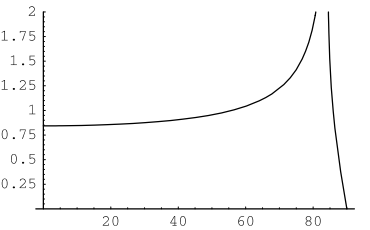

Figure 11. Graphs of I_θ/π and I'_θ/π for "fat" torus, $a/\rho = 0.9$.

7. *Weingarten surfaces*: A Weingarten surface is one for which a functional relationship $k_2 = F(k_1)$ holds between the principal curvatures k_1, k_2. The usual parametrization of Weingarten surfaces is slightly different from what we use above. Namely, one sets

$$h(r) = r = r(k_1) = r_0 \exp\left(\int_{1/r_0}^{k_1} \frac{\mathrm{d}\kappa_1}{F(\kappa_1)-\kappa_1}\right), \quad g(r) = \pm\int_{r_0}^{r} \frac{\rho k_1(\rho)\,\mathrm{d}\rho}{\sqrt{1-\rho^2 k_1^2(\rho)}}.$$

Here r_0 is the equatorial radius (F must satisfy several conditions, see [6]. In particular we assume $F(r_0^{-1}) \neq r_0^{-1}$). Since in that case the integrand in the expression for $r(k_1)$ just above is never zero, the function can be inverted so k_1 is made a function of r, which is the latitudinal radius. The quantity r is a reasonable choice for parametrizing the surface, which however it is not a parametrization of the form used above, since $r \neq 0$ at the equator, but more importantly, $h'(r_0) \neq 0$. However, if $u = g(r)$ is used as the parameter, so that

$$H(u) = g^{-1}(u), \qquad G(u) = u$$

then since $g'(1) = \infty$, $H'(0) = 0$, and the parametrization is of the requisite form. Explicit calculations as above for other manifolds are seldom possible. We can however, often determine the possible indices of closed geodesics. In particular, we can compute the result of Proposition 5. More generally, suppose, one has a parametrization $g(r)$ (not necessarily from above), leading to the reparametrization H and G. With this parametrization, one can compute the result of Proposition 5.

Proposition 7.

$$\lim_{c\to H_0} I_c = \frac{1}{\sqrt{r_0 F(r_0^{-1})}}\cdot$$

Proof: Note that

$$\lim_{c\to H_0} \frac{\pi\gamma_0}{\sqrt{-h_0 h_0''}} = \lim_{r\to r_0} \pi\sqrt{\frac{g'(r)\big(1+g'^2(r)\big)}{r g''(r)}}$$

because, since $u = g(r)$

$$\frac{\mathrm{d}}{\mathrm{d}r} = \frac{\mathrm{d}g}{\mathrm{d}r}\frac{\mathrm{d}}{\mathrm{d}u}$$

so that $H'(u)g'(r) = 1$ and

$$H''(u)g'^2(r) + H'(u)g''(r) = h''(u)g'^2(r) + g''(r)/g'(r) = 0.$$

For Weingarten surfaces, note that

$$g'(r) = \frac{r k_1(r)}{\sqrt{1 - r^2 k_1^2(r)}}, \qquad k_1'(r) = \frac{F(k_1) - k_1}{r}, \qquad k_1(r_0) = r_0^{-1}.$$

Substituting completes the proof.

For example, consider the Hopf surfaces, the Weingarten surfaces for which $F(k_1) = ck_1 - d$ [4]. See also [6, 7]. Note that if $d = 0$, the surfaces scale, that is, if the metric is scaled uniformly by a factor σ, the curvatures of the surface in the new metric obey the same functional relationship. See [5, p. 93] for profile curves in this case. Here we set $c \geq 1$, in which case, the Hopf surfaces are C^2. The result of Theorem 1 is immediate.

Appendix: Elliptic Integrals

$$\begin{aligned}
\prod(n\,|\,m) &= \int_0^{\pi/2} \frac{\mathrm{d}\theta}{(1-n\sin^2\theta)\sqrt{1-m\sin^2\theta}} \\
&= \int_0^{\pi/2} \frac{\mathrm{d}t}{(1-nt^2)\sqrt{(1-r^2)(1-mt^2)}} \\
&= \int_0^{K(m)} \frac{\mathrm{d}\varphi}{1-n\,\mathrm{cn}^2(\varphi,\sqrt{m})} \\
&= \frac{\pi}{2} F_1\left(\frac{1}{2};\frac{1}{2},1;m,n\right) \qquad \text{(Appell hypergeometric function)} \\
&= \frac{\pi}{2} F_{100}^{111}\left(\begin{matrix}\frac{1}{2};1;\frac{1}{2};\\ 1;;;\end{matrix} n,m\right) \qquad \text{(hypergeometric function of two variables)}
\end{aligned}$$

$$\begin{aligned}
K(m) &= \int_0^{\pi/2} \frac{\mathrm{d}\theta}{\sqrt{1-m\sin^2\theta}} = \int_0^1 \frac{\mathrm{d}t}{\sqrt{(1-mt^2)(1-t^2)}} \\
&= \prod(0\,|\,m) = \frac{\pi}{2}{}_2F_1\left(\frac{1}{2},\frac{1}{2};1;m\right)
\end{aligned}$$

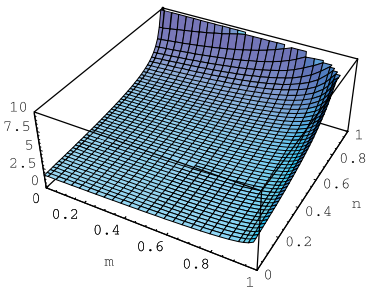

Figure A.1. Graph of the elliptic integral $\Pi(m\,|\,n)$.

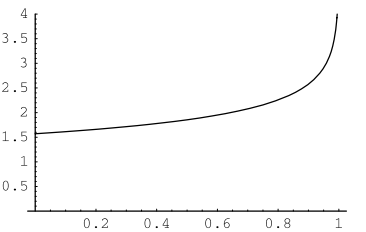

Figure A.2. Graph of the elliptic integral $K(m)$.

References

[1] Bliss G., *The Geodesic Lines On the Anchor Ring,* Ann. Math. **3** (1902)1–21.

[2] Byrd P. and Friedman M., *Handbook of Elliptic Integrals for Engineers and Physicists,* Second Edition, Springer, Berlin, 1971.

[3] Forsyth A., *Calculus of Variations,* Cambridge University Press, Cambridge, 1927.

[4] Hopf H., Über Flächen mit einer Relation zwischen den Hauptkrümmungen, Math. Nachr. **4** (1950/51) 232–249.

[5] Kühnel W., *Differential Geometry: Curves, Surfaces, Manifolds,* American Mathematical Society, Providence, RI, 2002.

[6] Kühnel W. and Steller M., *On Closed Weingarten Surfaces,* Monat. für Math. **146** (2005) 113–126.

[7] López R., *On Linear Weingarten Surfaces,* arXiv:math/0607748, 2006.

[8] Mladenov I. and Oprea J., *The Mylar Balloon Revisited,* Am. Math. Monthly **110** (2003) 761–784.

[9] Mladenov I. and Oprea J., *Unduloids and Their Closed Geodesics,* In: Geometry, Integrability and Quantization IV, Coral Press, Sofia, 2003, pp. 206–234.

[10] Mladenov I. and Oprea J., *The Mylar Balloon: New Viewpoints and Generalizations,* In: Geometry, Integrability and Quantization VII, SOFTEX, Sofia, 2006, pp. 246–263.

[11] Oprea J., *Differential Geometry and Its Applications,* Second Edition, Prentice Hall, New Jersey, 2004.

James C. Alexander
Department of Mathematics
Case Western Reserve University
10900 Euclid Avenue
Cleveland, OH 44106
USA
E-mail address:
james.alexander@case.edu